Structure, Stability, and Thermochemistry of the Fullerene Derivatives $C_{64}X_6$ (X = H, F, Cl)

Lei Xu, Xueguang Shao, and Wensheng Cai*

Department of Chemistry, Nankai University, Tianjin 300071, People's Republic of China

Received: June 18, 2009; Revised Manuscript Received: August 12, 2009

The geometrical structures, electronic properties, and stabilities of the unconventional fullerene derivatives $C_{64}X_6$ (X = H, F, Cl) have been systematically studied by the first-principle calculations based on the density functional theory. The fullerene derivatives 1911(2)-$C_{64}X_6$ generated from the pineapple-shaped $C_{64}X_4$ are predicted to possess the lowest energies. The other two X atoms are added to the carbon atoms with the highest local strain assessed by the pyramidalization angles. The calculations of the nucleus-independent chemical shifts suggest that the aromaticity of $C_{64}X_6$ affects the stability order of the derivative isomers. To address why $C_{64}H_6$ was not observed in the experimental study of Wang et al. (*J. Am. Chem. Soc.* **2006**, *128*, 6605) and if the halogenated derivatives $C_{64}X_6$ (X = F, Cl) can be synthesized, thermochemical analysis of the reaction $C_{64}X_4 + X_2 \rightarrow C_{64}X_6$ was also performed. The results indicate that the formation of $C_{64}H_6$ and $C_{64}Cl_6$ is not favored at high temperatures. The former may be a reason why $C_{64}H_6$ was not found in the experiment. In sharp contrast, the Gibbs free energy change to form $C_{64}F_6$ is found to be −23.29 kcal/mol at 2000 K, suggesting that this compound may be formed and detected in experiments. The NMR and IR spectra of 1911(2)-$C_{64}F_6$ are sequentially calculated and presented to facilitate future experimental identification.

1. Introduction

The geometry of fullerene is governed by the isolated pentagon rule (IPR),[1] which states that the most stable cage structures have every pentagon surrounded by five hexagons to minimize the steric strain resulting from the misalignment of the sp^2 hybrid orbitals on the fullerene surface. Except for I_h-C_{60},[2] all possible isomers of fullerenes with less than 70 carbon atoms disobey the IPR and, hence, are called unconventional fullerenes or non-IPR fullerenes. Compared to the normal fullerenes such as C_{60} and C_{70}, these unconventional fullerenes have also attracted significant scientific interest, because they are precursors of normal fullerenes in the growth process according to the "fullerene road" mechanism.[3−6] Investigations of the unconventional fullerenes are expected to provide valuable clues about how the fullerenes grow up.

Owing to the high strain of the unavoidable adjacent pentagons, the unconventional fullerenes are predicted to be highly unstable and difficult to isolate; however, they can be stabilized by forming endohedral or exohedral derivatives with other groups. Chemists are very interested in why and how these extremely unstable fullerenes are stabilized. Through encapsulation of small clusters (or atoms), some endohedral derivatives of the unconventional fullerenes, such as $Sc_2@C_{66}$,[7] $Sc_2C_2@C_{68}$,[8] and $Sc_3N@C_{68}$,[9] have been successfully synthesized and characterized. Further investigations[7−9] reveal that the electron transfer between the encapsulated cluster and the fullerene cage greatly releases the bond strain in the fused pentagons, hence increasing the stability of the endohedral fullerene derivatives. On both the theoretical and experimental fronts, a vast effort has been invested to study the exohedral chemical deriving of the unconventional fullerenes.[10−19] The structures and electronic properties of $C_{54}Cl_8$,[10] $C_{56}Cl_8$,[11] $C_{56}Cl_{10}$,[11] hept-$C_{62}X_2$,[12] $C_{64}X_4$,[13] and $C_{66}X_4$[14] (X = H, F, Cl, or Br) have been explored by using the density functional theory method. Through a graphite arc-discharge process modified by introducing carbon tetrachloride (CCl_4) in the helium atmosphere, Xie et al.[15] have successfully synthesized the first stable exohedral fullerene derivative $C_{50}Cl_{10}$ in milligram quantities. Recently, a new exohedral fullerene derivative $C_{64}H_4$[17] has also been isolated in milligram quantities using the arc-burning method by introducing methane, and no other C_{64}-based fullerides were observed in the product. Moreover, the similar $C_{64}Cl_4$[19] derivative has also been produced, and the $C_{64}F_4$[13] isomer was predicted to be more stable than the former two. The corresponding results also reveal that four X (X = H, Cl, F) atoms are covalently attached to the fused edges of three fused pentagons to form a stable pineapple-shaped structure, which is believed to essentially release the strain in the abutting-pentagons of C_{64}. Naturally, the following questions are raised from the above studies. Why are no other C_{64}-based fullerides, such as $C_{64}H_6$, found? Can the halogenated derivatives $C_{64}X_6$ (X = F, Cl) be synthesized and observed? What are the most stable structures of $C_{64}X_6$ and how are these derivatives stabilized?

To address these issues, in the present contribution, the first-principle density functional calculations were performed on the exohedral fullerene derivatives, $C_{64}X_6$ (X = H, F, Cl). The most stable structures and the factors contributing to the stability were discussed. Furthermore, the frequency calculation and thermochemical analysis of the most stable $C_{64}X_6$ isomers were carried out. The results are expected to explain why $C_{64}H_6$ was not found in the experiment of Wang et al.[17] and to give prediction of the possibility that the other two fullerene derivatives, viz., $C_{64}F_6$ and $C_{64}Cl_6$, can be observed in future experiments.

2. Methods

2.1. Generation of Initial Structures. In non-IPR fullerenes, the pentagon−pentagon fusion vertexes (PPFVs) are considered to be kinetically unstable. Among all 3465 C_{64} classical isomers generated by a spiral algorithm,[20,21] there are 4 isomers with

* Corresponding author: tel, +86-22-23503430; fax, +86-22-23502458; e-mail, wscai@nankai.edu.cn.

10.1021/jp905734n CCC: $40.75
Published on Web 09/16/2009

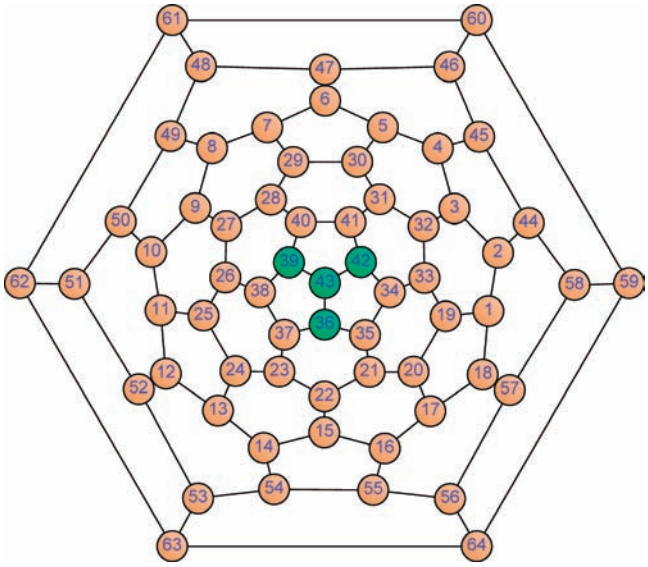

Figure 1. The Schlegel diagram with numbered carbon atoms of C_{64}: 1911. Attaching X atoms to the four pentagon−pentagon fusion vertexes (PPFVs) in dark green leads to the pineapple-shaped $C_{64}X_4$.

four PPFVs and 13 isomers with six PPFVs, while the others possess PPFV values larger than six. To fully stabilize C_{64} via exohedral addition, all of the kinetically unstable PPFV atoms need to be saturated sufficiently.[10,11,22] Hence, to identify the most stable $C_{64}X_6$ (X = H, F, Cl), only the isomers with four and six PPFVs are taken into account as the parent cages.

The $C_{64}X_6$ derivatives from all the 13 parent cages with six PPFVs were generated by simply adding six X atoms to all the PPFV carbons. Among the four parent cages with four PPFVs, C_{64}:1911 (numbering in spiral nomenclature, the corresponding Schlegel diagram is depicted in Figure 1) was reported to be the most favorable one for the $C_{64}X_4$ (X = H, F, Cl, Br) derivatives.[13,17,19] In these studies, the pineapple-shaped structure with C_{3v} symmetry was suggested for $C_{64}X_4$, all four PPFVs of which were saturated by four X atoms. Thus, C_{64}:1911 was also employed as a parent cage of $C_{64}X_6$ in this study. The initial isomers were generated from the pineapple-shaped structure of $C_{64}X_4$ by adding the other two X atoms to the active carbon atoms. In light of the theoretical investigations,[23,24] the active order of the carbon atoms in fullerene is 5/5/5 > 5/5/6 > 6/6/5 > 6/6/6: 5 and 6 denote pentagon and hexagon, respectively; 5/5/5 indicates the common vertex of triplet pentagons; 5/5/6 indicates the common vertex of two pentagons and one hexagon, and the rest may be deduced by analogy. The 5/5/5 and 5/5/6 carbon atoms have been saturated for the pineapple-shaped $C_{64}X_4$. Therefore, in this study, all the 6/6/5 carbon atoms and the 6/6/6 carbons nearby the three abutting pentagons are chosen as active carbon atoms for the addition of the other two X atoms. Among all the possible combinations, 33 different pairs of addition sites with higher symmetry were considered, yielding 33 different $C_{64}X_6$ isomers from the pineapple-shaped $C_{64}X_4$ (see Table S1 in the Supporting Information).

The other three parent cages with four PPFVs are C_{64}:3451, C_{64}:3452, and C_{64}:3457, bearing D_2, C_s, and C_2 symmetry, respectively (the corresponding Schlegel diagrams are depicted in Figure S1 in Supporting Information). According to the above generation method, we construct 45, 34, and 30 different $C_{64}X_6$ isomers with higher symmetry based on C_{64}:3451, C_{64}:3452, and C_{64}:3457, respectively (the attaching sites can also be seen in Table S1 in Supporting Information). These isomers are prescreened using the semiempirical PM3 method, and the top 10 PM3 low-energy isomers from each parent cage are selected for the further calculations. The total number of isomers of $C_{64}X_6$ investigated in the following, therefore, amounts to 76.

2.2. Geometry Optimization and Stability Analysis. All 76 initial structures of the fullerene derivatives $C_{64}X_6$ (X = H, F, Cl) were optimized using the HF[25]/3-21G method. On the basis of the results, some lower-energy isomers of each $C_{64}X_6$ were further refined at the B3LYP[26]/6-31G(d) level of theory to predict the lowest-energy isomers. Earlier studies[10−14,22,27,28] have demonstrated the reliability of the B3LYP method in fullerene chemistry. B3LYP/6-31G(d) calculations can also give a good prediction of the IR and NMR spectra of fullerene derivatives corresponding to the experimental data.[15,17]

The strain and aromatic effects to the stability of $C_{64}X_6$ isomers were analyzed. For the former purpose, the pyramidalization angles[29,30] of the possible addition sites on the pineapple-shaped structure of $C_{64}X_4$, which are used to assess the local strains, were calculated through π-orbital axis vector (POAV)[29,30] analysis. To estimate the aromatic character of the fullerene derivatives, the nucleus-independent chemical shifts (NICS),[31,32] were measured for the optimized geometries, by employing the gauge-including atomic orbital (GIAO)[33] B3LYP/6-31G(d) method.

2.3. Thermochemical Analysis of the Reaction to Form $C_{64}X_6$. Two assumed reaction routines were taken into account to evaluate the thermochemical stabilities of $C_{64}X_6$ derivatives.

$$C_{64} + 3X_2 \rightarrow C_{64}X_6 \quad (1)$$

$$C_{64}X_4 + X_2 \rightarrow C_{64}X_6 \quad (2)$$

The corresponding reaction energy at the B3LYP/6-31G(d) level of theory was estimated, which is defined as the total energy difference between product and reactant. The reaction energy per X_2 is used for comparison of eqs 1 and 2. Moreover, the harmonic vibrational frequency calculation and thermochemical analysis were performed on the most stable fullerene derivatives at the same B3LYP/6-31G(d) level, and the Gibbs free energy changes (ΔG) according to eq 2 were calculated to predict whether the $C_{64}X_6$ isomers can be obtained at high temperature. All the computations reported in this study were performed using the Gaussian 03 program package.[34]

3. Results and Discussions

3.1. Structures of $C_{64}X_6$ (X = H, F, Cl). The relative energies of all the 76 $C_{64}X_6$ (X = H, F, Cl) isomers at the HF/3-21G level are reported in Table 1. Apparently, the lower-energy structures are those generated from the pineapple-shaped $C_{64}X_4$ isomers, while the other derivatives are less stable. To obtain more accurate results, the five lowest-energy isomers from C_{64}:1911, the stable isomers from C_{64}:3451, C_{64}:3452, and C_{64}:3457, and the top four lower-energy $C_{64}X_6$ structures with six PPFVs were calculated at higher level of theory, B3LYP/6-31G(d). The relative energies, HOMO−LUMO gaps, and NICS values at the cage centers are shown in Table 2, and the most stable structures, 1911(2)-$C_{64}X_6$, are depicted in Figure 2. It would be apparent that the isomers generated from the pineapple-shaped $C_{64}X_4$ have not only relatively lower energies but also much larger HOMO−LUMO gaps. This indicates that the derivatives from the pineapple-shaped $C_{64}X_4$ are more stable in both thermodynamics and kinetic aspects. A careful look at a pineapple-shaped $C_{64}X_4$ structure shows that ignoring the four X atoms and four attaching

TABLE 1: Relative Energies (E_{rel}) of the 76 $C_{64}X_6$ (X = H, F, Cl) Isomers at the HF/3-21G Level of Theory

		E_{rel}[c] (kcal/mol)					E_{rel}[c] (kcal/mol)		
isomer[a]	N_{PPFV}[b]	$C_{64}H_6$	$C_{64}F_6$	$C_{64}Cl_6$	isomer[a]	N_{PPFV}[b]	$C_{64}H_6$	$C_{64}F_6$	$C_{64}Cl_6$
1911(2)	4	0.00[1]	0.00[1]	0.00[1]	3451(44)	4	65.45[39]	67.52[39]	62.75[46]
1911(1)	4	2.90[2]	3.14[2]	9.63[3]	3454	6	65.47[40]	69.12[41]	61.28[42]
1911(31)	4	7.16[3]	9.49[5]	28.62[13]	3452(14)	4	66.08[41]	69.46[42]	57.11[35]
1911(7)	4	8.88[4]	6.88[3]	12.13[4]	1911(9)	4	66.54[42]	63.46[35]	57.24[36]
1911(8)	4	10.41[5]	7.91[4]	3.16[2]	1911(15)	4	66.54[43]	63.46[36]	57.24[37]
3457(1)	4	15.60[6]	11.39[6]	14.33[5]	1911(4)	4	69.29[44]	69.60[43]	63.82[47]
1911(29)	4	21.09[7]	16.59[7]	16.06[6]	3451(6)	4	69.56[45]	80.38[60]	66.21[49]
1911(6)	4	27.28[8]	27.39[10]	27.27[11]	3457(28)	4	70.75[46]	73.08[49]	60.77[41]
1911(19)	4	27.76[9]	24.60[8]	24.79[8]	3452(4)	4	71.10[47]	70.28[45]	58.79[38]
3452(19)	4	28.84[10]	37.34[14]	24.29[7]	3451(16)	4	71.31[48]	79.20[57]	71.88[59]
1911(3)	4	29.46[11]	26.26[9]	26.60[10]	3457(27)	4	71.53[49]	74.97[51]	62.16[44]
1911(10)	4	33.89[12]	31.00[11]	25.61[9]	1911(17)	4	72.76[50]	73.82[50]	70.01[53]
1911(23)	4	36.94[13]	33.87[12]	28.50[12]	1629	6	73.20[51]	70.04[44]	68.86[51]
3457(3)	4	37.08[14]	39.22[15]	37.94[17]	3451(24)	4	73.26[52]	83.76[62]	70.87[55]
1911(16)	4	38.62[15]	35.14[13]	29.56[14]	3451(28)	4	73.37[53]	77.74[54]	75.62[62]
3457(15)	4	40.57[16]	45.72[19]	34.46[15]	3457(21)	4	75.84[54]	78.78[56]	65.33[48]
1911(20)	4	42.32[17]	40.70[16]	34.84[16]	3457(6)	4	76.10[55]	80.16[59]	78.27[64]
3452(17)	4	42.37[18]	50.87[23]	49.14[26]	1911(13)	4	76.11[56]	79.73[58]	70.37[54]
3452(6)	4	45.84[19]	53.20[25]	48.81[25]	3455	6	76.14[57]	77.83[55]	71.08[56]
1911(26)	4	46.05[20]	41.12[17]	38.00[18]	1911(25)	4	76.24[58]	75.60[52]	71.69[58]
3451(38)	4	47.63[21]	56.60[31]	43.61[20]	1911(27)	4	76.91[59]	75.87[53]	72.21[60]
3452(28)	4	49.63[22]	51.76[24]	47.84[23]	1911(5)	4	78.76[60]	55.41[27]	51.27[28]
1310	6	49.80[23]	46.54[20]	46.33[22]	3451(36)	4	79.38[61]	85.29[65]	71.29[57]
3457(30)	4	50.19[24]	55.78[29]	48.70[24]	3402	6	80.80[62]	84.07[63]	77.03[63]
1911(22)	4	50.72[25]	48.13[21]	42.24[19]	1911(12)	4	81.56[63]	72.04[48]	68.32[50]
1911(11)	4	52.13[26]	49.84[22]	43.84[21]	2730	6	82.06[64]	83.51[61]	79.68[65]
1911(33)	4	55.33[27]	44.38[18]	56.17[34]	3451(34)	4	83.81[65]	89.54[68]	75.30[61]
3451(40)	4	57.19[28]	64.40[38]	62.28[45]	3451(21)	4	86.86[66]	94.79[69]	81.06[66]
3452(15)	4	57.66[29]	57.12[32]	53.79[32]	1911(32)	4	86.96[67]	88.25[67]	95.53[71]
3452(30)	4	58.25[30]	68.50[40]	59.35[39]	2983	6	91.54[68]	85.80[66]	82.80[67]
1911(21)	4	59.72[31]	55.70[28]	50.87[27]	1911(28)	4	92.25[69]	84.93[64]	90.26[69]
1911(24)	4	60.35[32]	58.03[34]	51.60[29]	3423	6	94.02[70]	98.05[70]	90.97[70]
1911(30)	4	61.58[33]	55.25[26]	54.23[33]	3457(26)	4	95.60[71]	98.81[71]	85.52[68]
1911(14)	4	61.73[34]	57.69[33]	52.13[30]	3416	6	103.92[72]	109.16[72]	101.45[72]
3452(29)	4	62.49[35]	70.54[46]	61.43[43]	3424	6	104.66[73]	112.52[73]	103.82[73]
3457(14)	4	62.83[36]	64.38[37]	59.68[40]	3425	6	121.13[74]	123.02[74]	114.50[74]
3452(26)	4	64.04[37]	71.17[47]	69.23[52]	3428	6	127.14[75]	134.40[75]	126.51[75]
1911(18)	4	65.27[38]	56.36[30]	52.33[31]	3438	6	136.89[76]	136.14[76]	127.60[76]

[a] Code of parent fullerene numbering in spiral nomenclature.[20,21] (*n*) is used to distinguish different $C_{64}X_6$ isomers based on C_{64}:1911, C_{64}:3451, C_{64}:3452, and C_{64}:3457. [b] Number of pentagon−pentagon fusion vertexes (PPFV). [c] [*n*] indicates the stability order for each $C_{64}X_6$.

TABLE 2: Relative Energies (E_{rel} in kcal/mol), HOMO−LUMO Gaps (E_g in eV), and NICS Values (in ppm) at the Cage Centers for the 12 Selected $C_{64}X_6$ Isomers at the B3LYP/6-31G(d) Level of Theory[a]

		$C_{64}H_6$			$C_{64}F_6$			$C_{64}Cl_6$		
isomer	symmetry	E_{rel}	E_g	NICS	E_{rel}	E_g	NICS	E_{rel}	E_g	NICS
1911(2)	C_s	0.00[1]	2.704	−11.2	0.00[1]	2.732	−10.4	0.00[1]	2.733	−10.7
1911(31)	C_s	2.49[2]	2.543	−8.6	4.15[3]	2.604	−7.4			
1911(1)	C_s	3.19[3]	2.759	−11.2	2.77[2]	2.715	−10.4	9.73[4]	2.692	−10.5
1911(7)	C_1	9.70[5]	2.620	−8.9	7.73[5]	2.662	−8.7	12.09[5]	2.635	−8.8
1911(8)	C_s	11.46[6]	2.561	−7.5	9.29[6]	2.508	−8.0	1.69[2]	2.494	−7.9
1911(29)	C_s							15.53[6]	2.508	−7.9
3457(1)	C_2	9.13[4]	2.137	−9.4	5.84[4]	2.170	−8.3	7.94[3]	2.118	−8.4
3452(19)	C_s	25.25[7]	2.416	−13.5	29.45[8]	2.287	−12.0	17.46[7]	2.247	−12.4
3451(38)	C_2	33.72[9]	1.509	−13.0	38.38[9]	1.494	−11.0	26.23[9]	1.459	−11.8
1310	C_1	28.12[8]	1.351	−17.3	24.17[7]	1.304	−16.1	20.33[8]	1.303	−16.5
1629	C_s	43.55[10]	0.854	−12.5	39.89[10]	0.846	−13.7	36.10[10]	0.831	−13.8
3454	C_2	47.89[11]	1.798	−13.0	46.97[11]	1.773	−11.5	38.09[11]	1.737	−12.0
3455	C_1	49.57[12]	1.263	−11.1	47.69[12]	1.280	−8.3	39.19[12]	1.242	−9.0

[a] (*n*) and [*n*] stand for the same meaning as in Table 1.

carbon atoms, the remaining structure is similar to a perfect C_{60} molecule. This structural similarity may be the reason why the pineapple-shaped $C_{64}X_4$ can be synthesized in experiments,[17,19] and why the $C_{64}X_6$ generated from them are more stable.

3.2. Factors Contributing to the Stability of $C_{64}X_6$ (X = H, F, Cl). From Table 1, it can be found that although the electronegativities of H, F, and Cl are different, the stability order of $C_{64}X_6$ isomers is similar except for a few isomers such as 1911(31)-$C_{64}X_6$. This indicates that the charge transfer

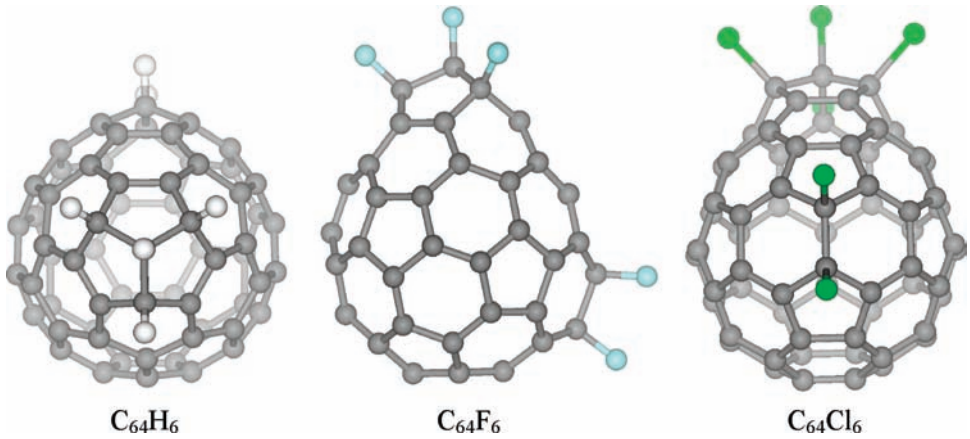

Figure 2. B3LYP/6-31G(d) optimized structures of the most stable fullerene derivatives 1911(2)-$C_{64}X_6$ from different directions.

TABLE 3: Pyramidalization Angles of the 12 Different sp^2 Carbon Atoms in the Pineapple-Shaped $C_{64}X_4$ (X = H, F, Cl)

carbon atom[a]	pyramidalization angle (deg)		
	$C_{64}H_4$	$C_{64}F_4$	$C_{64}Cl_4$
1, 5, 7, 11, 13, 17	11.4	11.5	11.5
2, 4, 8, 10, 14, 16	11.5	11.5	11.5
19, 20, 24, 25, 29, 30	10.6	10.5	10.6
21, 23, 26, 28, 31, 33	8.4	8.5	8.5
34, 35, 37, 38, 40, 41	7.5	7.6	7.4
44, 45, 49, 50, 54, 55	11.6	11.7	11.7
46, 48, 51, 53, 56, 58	11.8	11.8	11.8
59, 60, 61, 62, 63, 64	11.6	11.6	11.6
3, 9, 15	10.4	10.4	10.5
6, 12, 18	11.9	11.9	11.9
22, 27, 32	9.6	9.6	9.7
47, 52, 57	11.9	11.8	11.8

[a] Carbon atom number can be seen in Figure 1. Isoatoms due to the symmetry are listed in one set.

between the H, F, and Cl atoms and the fullerene cage affects the stability slightly. In 1911(31)-$C_{64}X_6$ derivatives, five X atoms are attached to one pentagon, as delineated in Figure S2 in the Supporting Information. The steric repulsion of the exohedral addends increases and, hence, lowers its stability as the atom volume increases for H, F, and Cl.

To probe the influence of the other two attaching sites in the pineapple-shaped $C_{64}X_4$, the corresponding geometries were first optimized at the B3LYP/6-31G(d) level, and then the pyramidalization angle was calculated for each carbon atom to assess its local strain. According to the structural symmetry (C_{3v}), only 12 different sp^2 carbon atoms are considered, and the results are presented in Table 3. The 12, 52 carbon atoms (denoted in Figure 1) possess the largest pyramidalization angles, suggestive of the highest local strain. Attaching X atoms to those sites can, hence, release the most energy, rationalizing the result of the energy calculations, wherein the two attaching sites of the most stable isomers, 1911(2)-$C_{64}X_6$, are 12 and 52. The 1911(31)-$C_{64}X_6$ isomers (attaching sites: 40, 41), however, are also very stable, although the pyramidalization angles of 40 and 41 carbon atoms are the smallest. This may be because adding two X atoms to 40 and 41 carbons only slightly alters the structures of the stable pineapple-shaped $C_{64}X_4$. From all the above, it can be summarized that adding X atoms to the sites with large pyramidalization angle or having little influence to the stable $C_{64}X_4$ both lead to stable $C_{64}X_6$ derivatives.

In addition, the NICS values at the cage center of the $C_{64}X_6$ derivatives were measured to probe their aromaticity, based on the idea that the more negative the NICS value, the more aromatic the structure. According to Table 2, the stability order of the five low-energy isomers generated from the pineapple-shaped $C_{64}X_4$ by and large correlates with their NICS values. This correlation also exists in the four less stable isomers with six PPFVs. It is, however, destroyed by applying to the 12 selected isomers, suggesting that NICS alone cannot explain the relative stabilities of the fullerene derivatives.

TABLE 4: The Reaction Energies per X_2 (E_{rea}) of Equations 1 and 2 for the Most Stable 1911(2)-$C_{64}X_6$ Isomers at the B3LYP/6-31G(d) Level of Theory[a]

	E_{rea} (kcal/mol)		
	$C_{64}H_6$	$C_{64}F_6$	$C_{64}Cl_6$
eq 1	−49.29	−132.06	−49.20
eq 2	−21.41	−99.47	−16.38

[a] For comparison, the B3LYP/6-31G(d) reaction energies per X_2 are calculated to be −63.22, −148.36, and −65.61 kcal/mol for the formation of the pineapple-shaped $C_{64}H_4$, $C_{64}F_4$, and $C_{64}Cl_4$, respectively.

3.3. Thermochemical Analysis of $C_{64}X_6$ (X = H, F, Cl). The reaction energies per X_2 of eq 1 for the formation of the most stable 1911(2)-$C_{64}X_6$ isomers are gathered in Table 4. It would appear that the reactions are highly exothermic, mainly because binding six H, F, or Cl atoms releases much of the strain of the C_{64} cage, particularly in the case of F. Can these $C_{64}X_6$ compounds be formed by experiments? Compared to the well-known decachlorofullerene $C_{50}Cl_{10}$ (reported to be −50.7 kcal/mol),[22] the reaction energy for $C_{64}H_6$ and $C_{64}Cl_6$ is approximate, and for $C_{64}F_6$ much higher. Thus, the synthesis of 1911(2)-$C_{64}X_6$ derivatives seems feasible. Yet, in the experimental study of Wang et al.,[17] $C_{64}H_6$ had not been observed in the products. To explain this phenomenon, the reaction energies of $C_{64} + 2X_2 \rightarrow C_{64}X_4$ were also estimated (see the footnote of Table 4). The latter reactions are suggested to be more favored than eq 1. Furthermore, the reaction energies of eq 2 for the formation of 1911(2)-$C_{64}X_6$ from 1911-$C_{64}X_4$ were also calculated. The results in Table 4 show that the reaction energy of eq 2 is remarkably lower than that of eq 1, due to the high stability of the pineapple-shaped $C_{64}X_4$. This step of reaction, however, is still found to be exothermic, which cannot explain the experiment. As the temperature of the arc-burning experiment is very high, the contribution of the entropy, therefore, should be taken into account. This is implemented by estimating the Gibbs free energy change (ΔG) of eq 2 at a temperature of 2000−3000K and a pressure of 500 Torr, which are used to mimic the conditions of the arc-burning experiment.[17]

TABLE 5: The Gibbs Free Energy Change (ΔG) of Equation 2 at 2000, 2500, and 3000 K for the Most Stable 1911(2)-$C_{64}X_6$ Isomers at the B3LYP/6-31G(d) Level of Theory

	ΔG (kcal/mol)		
temperature (K)	$C_{64}H_6$	$C_{64}F_6$	$C_{64}Cl_6$
2000	50.99	−23.29	56.74
2500	67.25	−5.92	73.39
3000	83.25	11.15	89.73

The calculated ΔG at the B3LYP/6-31G(d) level is shown in Table 5. Clearly, ΔG is very positive for the reaction of $C_{64}H_6$ and $C_{64}Cl_6$ due to the effect of entropy, indicating that it is disfavored to form them at the high temperature. This may be the reason why no $C_{64}H_6$ fulleride was found in the experiment of ref 17. Inspiringly, for the formation of $C_{64}F_6$, ΔG is negative at the temperature below 2500 K, even at 3000 K it is just a small positive value. The reason may be the reaction of adding F atoms is more exothermic than that of Cl or H atoms. These results strongly suggest that at variance with $C_{64}H_6$ and $C_{64}Cl_6$, the 1911(2)-$C_{64}F_6$ isomer can probably be formed and observed along with the pineapple-shaped $C_{64}F_4$ in the arc-discharge experiments.

3.4. Spectroscopy of the 1911(2)-$C_{64}F_6$ Derivative. To provide a verifying basis for the experimental identification of 1911(2)-$C_{64}F_6$ isomer, we have calculated the NMR spectra at the GIAO-B3LYP/6-31G(d) level of theory and IR spectra at the B3LYP/6-31G(d) level of theory, based on the optimized geometry at the same level. The ^{13}C chemical shifts of 1911(2)-$C_{64}F_6$ are computed relative to C_{60} and converted to the TMS (tetramethylsilane) scale using the experimental value for C_{60} ($\delta = 142.7$ ppm).[35] There are 35 different carbon atoms (29×2; 6×1) according to the symmetry (C_s), and thus 35 different lines are shown in Figure 3. $a \times b$ represents a different types, and in one type, there are b symmetrical equivalent atoms. The calculated ^{13}C NMR spectra can be easily divided into two regions. There are 30 peaks with chemical shifts from 124.67 to 152.54 ppm in the left region, ascribed to the 58 sp^2 (28×2; 2×1) carbon atoms, 28 of which have the same intensity, and the other two have the half of the intensity. Five peaks appear in the right region with chemical shifts from 99.34 to 109.22 ppm, corresponding to the six sp^3 (1×2; 4×1) carbon atoms.

Figure 4 gives the calculated IR spectra of 1911(2)-$C_{64}F_6$ isomer. The most intensive peak is located at 1063 cm^{-1}, corresponding to the C−F stretching at the attaching sites 12, 52. The neighbored peaks (from 1000 to 1200 cm^{-1}) are also very intensive, mainly related to the other C−F stretching modes, and the other lower intensive peaks correspond to the cage breathing and C−C stretching modes. These results are expected to be helpful for experimental characterization in the future.

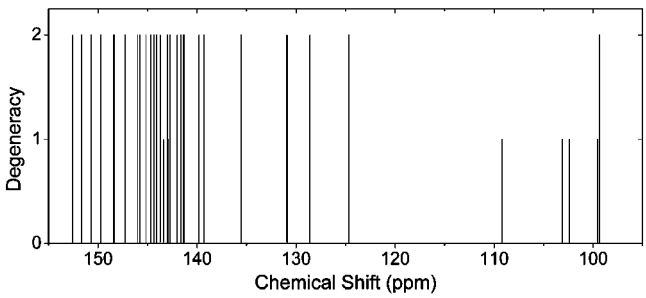

Figure 3. ^{13}C NMR spectra of the 1911(2)-$C_{64}F_6$ fullerene derivative.

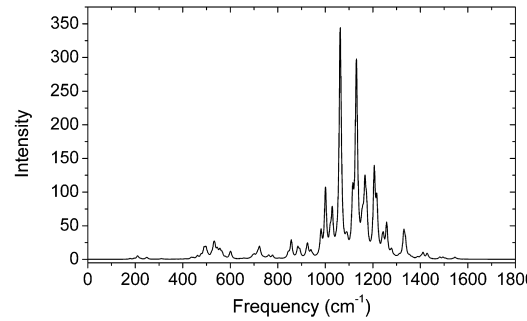

Figure 4. IR spectra of the 1911(2)-$C_{64}F_6$ fullerene derivative, which are scaled by a factor of 0.9613.

4. Conclusions

A systematic density functional investigation has been performed on the structures and stabilities of the unconventional fullerene derivatives $C_{64}X_6$ (X = H, F, Cl). The predicted most stable derivatives are 1911(2)-$C_{64}X_6$ generated from the pineapple-shaped $C_{64}X_4$ isomers. The structural similarity of the pineapple-shaped motif to the C_{60} molecule may be an important contribution to the stabilization of the $C_{64}X_6$ isomers generated from it. On the basis of this structural motif, the pair of carbon atoms with the largest local strain is considered to be the most favored addition sites. The stability of 1911(2)-$C_{64}X_6$ can also be ascribed to the significant release of strain by adding the other two X atoms at these two sites. Further analysis of the aromaticity through the NICS value shows that the former makes a positive contribution to the most stable 1911(2)-$C_{64}X_6$ isomers, although it is not a dominating factor to affect the relative stability of all the $C_{64}X_6$ isomers. Thermochemical analysis was also implemented on the most stable 1911(2)-$C_{64}X_6$. The results show that although the reaction is exothermic, the formation of $C_{64}H_6$ and $C_{64}Cl_6$ is disfavored at the high temperature, due to the effect of entropy. This can be considered as the reason why $C_{64}H_6$ was not found in the experiments. At variance with these two derivatives, the reaction to form $C_{64}F_6$ is shown to be highly exothermic, moreover, the corresponding Gibbs free energy change for adding two F atoms is found to be negative at the temperature below 2500 K. These results strongly suggest that $C_{64}F_6$ can probably be formed and observed in the arc-discharge experiments, besides $C_{64}F_4$. Finally, the NMR and IR spectra of 1911(2)-$C_{64}F_6$ are predicted to provide a verifying basis for the experimental identification.

Acknowledgment. This study is supported by National Natural Science Foundation of China (Nos. 20835002 and 20873066) and Nankai University ISC.

Supporting Information Available: Tables of fullerene derivatives $C_{64}X_6$ generated from the four parent cages with four PPFVs and the corresponding two attaching sites, Schlegel diagrams with numbered carbon atoms of C_{64}:3451, C_{64}:3452, and C_{64}:3457, general view of the structure of 1911(31)-$C_{64}X_6$ derivatives, and simulated IR spectra of C_{60} at the B3LYP/6-31G(d) level for the comparison with the experimental data. This information is available free of charge via the Internet at http://pubs.acs.org.

References and Notes

(1) Kroto, H. W. *Nature* **1987**, *329*, 529–531.
(2) Kroto, H. W.; Heath, J. R.; Obrien, S. C.; Curl, R. F.; Smalley, R. E. *Nature* **1985**, *318*, 162–163.
(3) Smalley, R. E. *Acc. Chem. Res.* **1992**, *25*, 98–105.

(4) Heath, J. R. *Nature* **1998**, *393*, 730–731.
(5) Shvartsburg, A. A.; Hudgins, R. R.; Dugourd, P.; Gutierrez, R.; Frauenheim, T.; Jarrold, M. F. *Phys. Rev. Lett.* **2000**, *84*, 2421–2424.
(6) Bates, K. R.; Scuseria, G. E. *J. Phys. Chem. A* **1997**, *101*, 3038–3041.
(7) Wang, C. R.; Kai, T.; Tomiyama, T.; Yoshida, T.; Kobayashi, Y.; Nishibori, E.; Takata, M.; Sakata, M.; Shinohara, H. *Nature* **2000**, *408*, 426–427.
(8) Shi, Z. Q.; Wu, X.; Wang, C. R.; Lu, X.; Shinohara, H. *Angew. Chem., Int. Ed.* **2006**, *45*, 2107–2111.
(9) Stevenson, S.; Fowler, P. W.; Heine, T.; Duchamp, J. C.; Rice, G.; Glass, T.; Harich, K.; Hajdu, E.; Bible, R.; Dorn, H. C. *Nature* **2000**, *408*, 427–428.
(10) Gao, X. F.; Zhao, Y. L. *J. Comput. Chem.* **2007**, *28*, 795–801.
(11) Chen, D. L.; Tian, W. Q.; Feng, J. K.; Sun, C. C. *ChemPhysChem* **2007**, *8*, 2386–2390.
(12) Sun, L. L.; Tang, S. W.; Chang, Y. F.; Wang, Z. L.; Wang, R. S. *J. Comput. Chem.* **2008**, *29*, 2631–2635.
(13) Yan, Q. B.; Zheng, Q. R.; Su, G. *J. Phys. Chem. C* **2007**, *111*, 549–554.
(14) Yan, Q. B.; Zheng, Q. R.; Su, G. *Carbon* **2007**, *45*, 1821–1827.
(15) Xie, S. Y.; Gao, F.; Lu, X.; Huang, R. B.; Wang, C. R.; Zhang, X.; Liu, M. L.; Deng, S. L.; Zheng, L. S. *Science* **2004**, *304*, 699–699.
(16) Troshin, P. A.; Avent, A. G.; Darwish, A. D.; Martsinovich, N.; Abdul-Sada, A. K.; Street, J. M.; Taylor, R. *Science* **2005**, *309*, 278–281.
(17) Wang, C. R.; Shi, Z. Q.; Wan, L. J.; Lu, X.; Dunsch, L.; Shu, C. Y.; Tang, Y. L.; Shinohara, H. *J. Am. Chem. Soc.* **2006**, *128*, 6605–6610.
(18) Tan, Y. Z.; Han, X.; Wu, X.; Meng, Y. Y.; Zhu, F.; Qian, Z. Z.; Liao, Z. J.; Chen, M. H.; Lu, X.; Xie, S. Y.; Huang, R. B.; Zheng, L. S. *J. Am. Chem. Soc.* **2008**, *130*, 15240–15241.
(19) Han, X.; Zhou, S. J.; Tan, Y. Z.; Wu, X.; Gao, F.; Liao, Z. J.; Huang, R. B.; Feng, Y. Q.; Lu, X.; Xie, S. Y.; Zheng, L. S. *Angew. Chem., Int. Ed.* **2008**, *47*, 5340–5343.
(20) Manolopoulos, D. E.; May, J. C.; Down, S. E. *Chem. Phys. Lett.* **1991**, *181*, 105–111.
(21) Fowler, P. W.; Manolopoulos, D. E. *An Atlas of Fullerenes*; Oxford University Press: Oxford, 1995.
(22) Lu, X.; Chen, Z. F.; Thiel, W.; Schleyer, P. V.; Huang, R. B.; Zheng, L. S. *J. Am. Chem. Soc.* **2004**, *126*, 14871–14878.
(23) Xiao, J. M.; Lin, M. H.; Chiu, Y. N.; Fu, M. Z.; Lai, S. T.; Li, N. N. *J. Mol. Struct. (THEOCHEM)* **1998**, *428*, 149–154.
(24) Lin, M. H.; Chiu, Y. N.; Xiao, J. M. *J. Mol. Struct. (THEOCHEM)* **1999**, *489*, 109–117.
(25) Roothaan, C. C. J. *Rev. Mod. Phys.* **1951**, *23*, 69–89.
(26) Becke, A. D. *J. Chem. Phys.* **1993**, *98*, 5648–5652.
(27) Cioslowski, J.; Rao, N.; Moncrieff, D. *J. Am. Chem. Soc.* **2000**, *122*, 8265–8270.
(28) Chen, D. L.; Tian, W. Q.; Feng, J. K.; Sun, C. C. *ChemPhysChem* **2008**, *9*, 454–461.
(29) Haddon, R. C. *J. Am. Chem. Soc.* **1986**, *108*, 2837–2842.
(30) Haddon, R. C. *Acc. Chem. Res.* **1988**, *21*, 243–249.
(31) Schleyer, P. v. R.; Maerker, C.; Dransfeld, A.; Jiao, H.; Hommes, N. J. R. v. E. *J. Am. Chem. Soc.* **1996**, *118*, 6317–6318.
(32) Chen, Z. F.; Wannere, C. S.; Corminboeuf, C.; Puchta, R.; Schleyer, P. v. R. *Chem. Rev.* **2005**, *105*, 3842–3888.
(33) Wolinski, K.; Hinton, J. F.; Pulay, P. *J. Am. Chem. Soc.* **1990**, *112*, 8251–8260.
(34) Frisch, M. J.; Trucks, G. W.; Schlegel, H. B.; Scuseria, G. E.; Robb, M. A.; Cheeseman, J. R.; Montgomery, J. A., Jr.; Vreven, T.; Kudin, K. N.; Burant, J. C.; Millam, J. M.; Iyengar, S. S.; Tomasi, J.; Barone, V.; Mennucci, B.; Cossi, M.; Scalmani, G.; Rega, N.; Petersson, G. A.; Nakatsuji, H.; Hada, M.; Ehara, M.; Toyota, K.; Fukuda, R.; Hasegawa, J.; Ishida, M.; Nakajima, T.; Honda, Y.; Kitao, O.; Nakai, H.; Klene, M.; Li, X.; Knox, J. E.; Hratchian, H. P.; Cross, J. B.; Adamo, C.; Jaramillo, J.; Gomperts, R.; Stratmann, R. E.; Yazyev, O.; Austin, A. J.; Cammi, R.; Pomelli, C.; Ochterski, J. W.; Ayala, P. Y.; Morokuma, K.; Voth, G. A.; Salvador, P.; Dannenberg, J. J.; Zakrzewski, V. G.; Dapprich, S.; Daniels, A. D.; Strain, M. C.; Farkas, O.; Malick, D. K.; Rabuck, A. D.; Raghavachari, K.; Foresman, J. B.; Ortiz, J. V.; Cui, Q.; Baboul, A. G.; Clifford, S.; Cioslowski, J.; Stefanov, B. B.; Liu, G.; Liashenko, A.; Piskorz, P.; Komaromi, I.; Martin, R. L.; Fox, D. J.; Keith, T.; Al-Laham, M. A.; Peng, C. Y.; Nanayakkara, A.; Challacombe, M.; Gill, P. M. W.; Johnson, B.; Chen, W.; Wong, M. W.; Gonzalez, C.; Pople, J. A. *Gaussian 03, Revision C.02*; Gaussian, Inc.: Wallingford, CT, 2004.
(35) Taylor, R.; Hare, J. P.; Abdul-Sada, A. K.; Kroto, H. W. *J. Chem. Soc., Chem. Commun.* **1990**, 1423–1425.

JP905734N